Appendix B2
Supplemental Water Supply Data and Methods

Appendix B2 — Supplemental Water Supply Data and Methods

This appendix provides supplemental information related to the water supply data and methods discussed in the Technical Report. As discussed in the Technical Report, the assessment of historical and future supply conditions focused on four main groups of water supply indicators: climate, hydrologic processes, climate teleconnections, and streamflow. Although the primary indicator of water supply in the Colorado River Basin (Basin) is streamflow, a fundamental understanding of the processes that influence the quantity, location, and timing of streamflow is beneficial. Additional detail on the methods used to assess these indicators for water supply is supplied in this appendix.

Table B2-1 summarizes the water supply indicators evaluated as part of the Water Supply Assessment. In addition, the table provides the relevance of the particular parameter for the Colorado River Basin Water Supply and Demand Study (Study), temporal and spatial scales considered, and analysis methods. Table B2-2 summarizes the data sources considered in the evaluation of each of the water supply indicators. The subsequent sections provide further detail on the data and methods under each of the four water supply indicator groups.

TABLE B2-1
Summary of the Water Supply Indicators for the Water Supply Assessment

Water Supply Indicator	Relevance	Temporal Scale	Spatial Scale	Method of Analysis	Method of Display
CLIMATE					
Temperature	Identification of trends in climate patterns	Monthly, Seasonal, Annual, Decadal	Grid cell, Select Watersheds, and Basin-wide	Statistical analysis of trends and variability	Spatial analysis and visualization
Precipitation	Identification of trends in climate patterns	Monthly, Seasonal, Annual, Decadal	Grid cell, Select Watersheds, and Basin-wide	Statistical analysis of trends and variability	Spatial analysis and visualization
HYDROLOGIC PROCESSES					
Runoff	Identification of changes in runoff processes; identification of "productive" watersheds	Monthly, Seasonal, Annual, Decadal	Grid cell, Select Watersheds, and Basin-wide	Calculated as unit runoff; statistics to be generated	Spatial analysis and visualization
Evapotrans-piration (ET)	Identification of changes in natural losses; identification of "water stressed" watersheds	Monthly, Seasonal, Annual, Decadal	Grid cell, Select Watersheds, and Basin-wide	Calculated as unit actual ET; statistics to be generated	Spatial analysis and visualization

TABLE B2-1
Summary of the Water Supply Indicators for the Water Supply Assessment

Water Supply Indicator	Relevance	Temporal Scale	Spatial Scale	Method of Analysis	Method of Display
Snowpack Accumulation and Snowmelt	Identification of spatial changes in snowpack development and timing of melt	Monthly, Seasonal, Annual, Decadal	Grid cell, Select Watersheds, and Basin-wide	Calculated as unit snow water equivalent (SWE); peak and timing	Spatial analysis and visualization
Soil Moisture	Identification of causes of drought and severe drying conditions; identification of watersheds most impacted	Monthly, Seasonal, Annual, Decadal	Grid cell, Select Watersheds, and Basin-wide	Calculated as percentage of maximum	Spatial analysis and visualization
CLIMATE TELECONNECTIONS					
El Niño – Southern Oscillation (ENSO)	Identify changes in teleconnections and influence on regional climate; identify relationship between long-term and shorter-term climate indices	Season, Annual, Decadal	Global/ Regional	Statistical analysis of correlation between indicator and streamflow	Correlation plots and statistics
Pacific Decadal Oscillation (PDO)	Identify changes in teleconnections and influence on regional climate; identify relationship between long-term and shorter-term climate indices	Annual, Decadal	Global/ Regional	Statistical analysis of correlation between indicator and streamflow	Correlation plots and statistics
Atlantic Multi-decadal Oscillation (AMO)	Identify changes in teleconnections and influence on regional climate; identify relationship between long-term and shorter-term climate indices	Annual, Decadal	Global/ Regional	Qualitative discussion	Qualitative discussion
STREAMFLOW					
Intervening and Total Natural Flows at 29 Basin Locations	Identification of changes in streamflow trends and variability	Monthly; Annual; 1-, 3-, 5-, 10-year; and multi-decadal	Accumulated Flow at Point	Statistical analysis of trends and variability; drought and surplus statistics	Table and box-whisker of statistics, Basin-scale maps

TABLE B2-2
Sources of Data Used for the Water Supply Assessment

Parameter	Description	Data Source
CLIMATE INDICATORS		
Historical Temperature and Precipitation	Historical gridded temperature and precipitation at 1/8th-degree resolution for the period of 1950–1999. Extension through 2005 was not documented.	Maurer et al., 2002 (http://www.engr.scu.edu/~emaurer/data.shtml)
Future Temperature and Precipitation Projections	A total of 112 future monthly temperature and precipitation projections based on Intergovernmental Panel on Climate Change (IPCC) Fourth Assessment Report (IPCC, 2007) emission scenarios, subsequently bias corrected, and statistically downscaled to 1/8th-degree resolution for the period of 1950–2099.	Maurer et al., 2007 (http://gdo-dcp.ucllnl.org/downscaled_cmip3_projections/)
HYDROLOGIC PROCESS INDICATORS		
ET, Runoff, SWE, Soil Moisture	Variable Infiltration Capacity (VIC)-simulated hydrologic fluxes and grid cell storage terms driven by observed climatology (1950–2005) and 112 future climate projections (1950–2099).	Bureau of Reclamation (Reclamation), 2011
Snowpack	Point snow water equivalent from late 1970s to present from the snow-telemetry (SNOTEL) network.	National Resources Conservation Service, 2011 (http://www.wcc.nrcs.usda.gov/snow/)
TELECONNECTION INDICATORS		
ENSO	Monthly Southern Oscillation Index (SOI) for January 1866 through March 2010.	University of East Anglia Climatic Research Unit , 2010 (http://www.cru.uea.ac.uk/cru/data/soi/)
PDO	Monthly PDO indices for January 1900 through January 2010.	Joint Institute for the Study of the Atmosphere and Ocean, 2010 (http://jisao.washington.edu/pdo/)
STREAMFLOW INDICATORS		
Observed Streamflow used in the Observed Resampled Scenario	Natural streamflow for the period of 1906–2007 for the 29 streamflow locations commonly used for Reclamation planning.	Prairie and Callejo, 2005; Reclamation, 2010
Paleo Reconstructed Streamflow used in the Paleo Resampled Scenario	Reconstructed natural streamflows for the period 762–2005 at 29 locations derived from ecologically contrasting tree-ring sites in the southern Colorado Plateau during the past 2 millennia.	Reclamation, 2010; Meko et al., 2007
Paleo Conditioned Streamflow used in the Paleo Conditioned Scenario	Blended paleo streamflow states with observed streamflow magnitudes at 29 locations.	Prairie et al., 2008
Future Streamflow Projections used in the Downscaled General Circulation Model (GCM) Projected Scenario	VIC-simulated runoff and routed streamflow at 29 locations driven by 112 future climate projections for the period 1950–2099.	Reclamation, 2011

1.0 Climate

1.1 Historical Climate

Gridded observed climate data for the period from 1950 to 1999, as developed by Maurer et al. (2002), were downloaded via the Internet from Santa Clara University (http://www.engr.scu.edu/~emaurer/data.shtml). The data are stored in network common data format (netCDF) at 1/8th-degree resolution and contain daily temperature (minimum and maximum), precipitation, and wind speed values for the contiguous United States. Subsequent to the Maurer et al. (2002) data, the gridded dataset was extended to 2005 using identical methods. The temperature and precipitation data were processed into monthly average temperature and monthly total precipitation to facilitate comparisons. The monthly, seasonal, and annual statistics were computed for each parameter and for each grid cell for the period 1971 to 2000 to facilitate comparisons to projected future conditions. This 1971 to 2000 historical base period was selected as the most current 30-year climatological period at the time of the Study, as described by the National Oceanic and Atmospheric Administration (NOAA) (2010), and was used as the basis for comparing to future climate projections[1].

1.2 Projections of Future Climate

Future climate change projections are made primarily on the basis of General Circulation Model (GCM) simulations under a range of future emission scenarios. A total of 112 future climate projections used in the IPCC Fourth Assessment Report, subsequently transformed to a local scale through bias correction and spatial downscaling (BCSD), were obtained from the Lawrence Livermore National Laboratory under the World Climate Research Program's (WCRP) Coupled Model Intercomparison Project Phase 3 (CMIP3). This archive contains climate projections generated from 16 different GCMs developed by national climate centers and for *Special Report on Emissions Scenarios* emission scenarios A2, A1B, and B1. These projections have been bias corrected and spatially downscaled to 1/8th-degree (~12-kilometer) resolution over the contiguous United States through methods described in detail in Wood et al. (2002; 2004) and Maurer (2007).

1.2.1 Emission Scenarios

In 2000, IPCC published the SRES scenarios that described a family of six emission scenarios to condition GCMs (IPCC, 2000). The emissions scenarios are defined by alternative future development pathways, covering a wide range of demographic, economic, and technological driving forces and resulting greenhouse gas (GHG) emissions. The GHG emissions associated with each scenario are shown in figure B2-1.

[1] A new 30-year historical base period (1981 to 2010) was issued by NOAA on July 1, 2011.

FIGURE B2-1
Scenarios for GHG Emissions from 2000–2100 in the Absence of Additional Climate Policies
Units on the y-axis are billon tons of total annual emissions in equivalent carbon dioxide units.

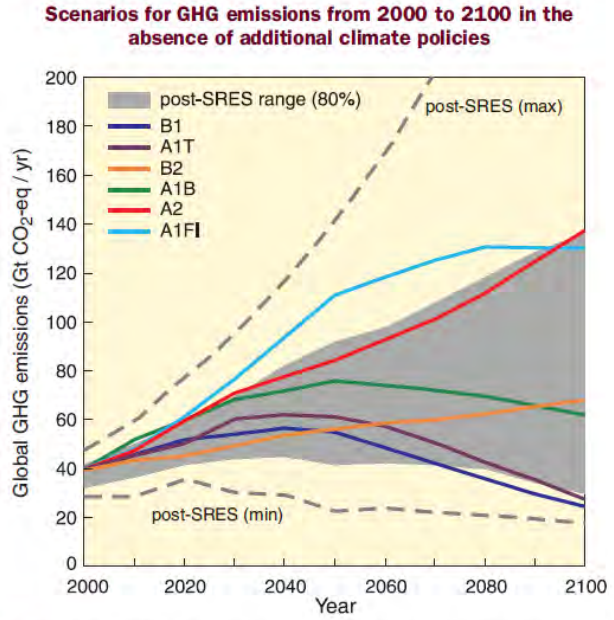

Figure 3.1. Global GHG emissions (in $GtCO_2$-eq per year) in the absence of additional climate policies: six illustrative SRES marker scenarios (coloured lines) and 80th percentile range of recent scenarios published since SRES (post-SRES) (gray shaded area). Dashed lines show the full range of post-SRES scenarios. The emissions include CO_2, CH_4, N_2O and F-gases. {WGIII 1.3, 3.2, Figure SPM.4}

Source: (IPCC, 2007)

Of the six emission scenarios included in the IPCC Fourth Assessment Report (IPCC, 2007), three were selected to drive the CMIP3 multi-model dataset—A2 (high), A1B (medium), and B1 (low). The A2 scenario is representative of high population growth, slow economic development, and slow technological change. It is characterized by a continuously increasing rate of GHG emissions and features the highest annual emissions rates of any scenario by the end of the 21st Century. The A1B scenario features a global population that peaks mid-century and rapid introduction of new and more-efficient technologies balanced across both fossil- and non-fossil-intensive energy sources. As a result, GHG emissions in the A1B scenario peak around mid-century. Lastly, the B1 scenario describes a world with rapid changes in economic structures toward a service and information economy. GHG emission rates in this scenario peak prior to mid-century and are generally the lowest of the scenarios. The best estimates of global temperature change during the 21st Century for each of the A2, A1B, and B1 scenarios are 3.4, 2.8, and 1.8 degrees Celsius (°C), respectively[2] (IPCC, 2007) as shown in Figure B2-2.

[2] Temperature change reflects the difference between the global average in the 2090 to 2099 period relative to the global average in the 1980 to 1999 period.

FIGURE B2-2
Projections of Surface Temperatures for the Selected GHG Emissions Scenarios from 2000–2100

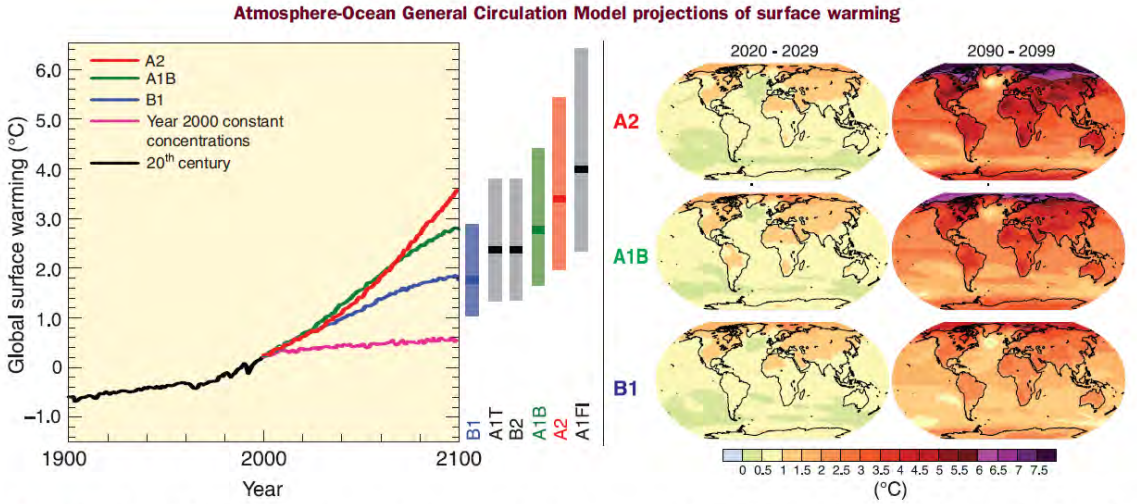

Figure 3.2. ***Left panel:*** *Solid lines are multi-model global averages of surface warming (relative to 1980-1999) for the SRES scenarios A2, A1B and B1, shown as continuations of the 20th century simulations. The orange line is for the experiment where concentrations were held constant at year 2000 values. The bars in the middle of the figure indicate the best estimate (solid line within each bar) and the* likely *range assessed for the six SRES marker scenarios at 2090-2099 relative to 1980-1999. The assessment of the best estimate and* likely *ranges in the bars includes the Atmosphere-Ocean General Circulation Models (AOGCMs) in the left part of the figure, as well as results from a hierarchy of independent models and observational constraints.* ***Right panels:*** *Projected surface temperature changes for the early and late 21st century relative to the period 1980-1999. The panels show the multi-AOGCM average projections for the A2 (top), A1B (middle) and B1 (bottom) SRES scenarios averaged over decades 2020-2029 (left) and 2090-2099 (right). {WGI 10.4, 10.8, Figures 10.28, 10.29, SPM}*

Source: (IPCC, 2007)

1.2.2 General Circulation Models

The CMIP3 multi-model dataset consists of 112 unique climate projections. Sixteen GCMs were coupled with the three emissions scenarios described previously to generate these projections. Many of the GCMs were simulated multiple times for the same emission scenario due to differences in starting climate system state or initial conditions, so the number of available projections is greater than simply the product of GCMs and emission scenarios. Table B2-3 summarizes the GCMs, initial conditions (specified by the run numbers in the A2, A1B, and B1 columns), and emissions scenario combinations (A2, A1B, and B1) featured in the CMIP3 dataset. Initial conditions (initial atmosphere and ocean conditions used in a GCM simulation) for the 21st Century are defined by the 20th Century "control" simulation. A description of the 20th Century "control" simulations corresponding to each GCM simulation in table B2-3 can be found at http://www-pcmdi.llnl.gov/ipcc/standard_output.html#Experiments.

TABLE B2-3
WCRP CMIP3 Multi-Model Dataset GCMs, Initial Conditions, and Emissions Scenarios

Modeling Group, Country	WCRP CMIP3 I.D.	A2	A1B	B1	Primary Reference
Bjerknes Center for Climate Research, Norway	BCCR-BCM2.0	1	1	1	Furevik et al., 2003
Canadian Center for Climate Modeling and Analysis, Canada	CGCM3.1 (T47)	1...5	1...5	1...5	Flato and Boer, 2001
Meteo-France/Center National de Recherches Meteorologiques, France	CNRM-CM3	1	1	1	Salas-Melia et al., 2005
CSIRO Atmospheric Research, Australia	CSIRO-Mk3.0	1	1	1	Gordon et al., 2000
U.S. Dept. of Commerce/NOAA/Geophysical Fluid Dynamics Laboratory, United States	GFDL-CM2.0	1	1	1	Delworth et al., 2006
U.S. Dept. of Commerce/NOAA/Geophysical Fluid Dynamics Laboratory, United States	GFDL-CM2.1	1	1	1	Delworth et al., 2006
National Aeronautics and Space Administration/Goddard Institute for Space Studies, United States	GISS-ER	1	2, 4	1	Russell et al., 2000
Institute for Numerical Mathematics, Russia	INM-CM3.0	1	1	1	Diansky and Volodin, 2002
Institut Pierre Simon Laplace, France	IPSL-CM4	1	1	1	Institut Pierre Simon Laplace, 2005
Center for Climate System Research (The University of Tokyo), National Institute for Environmental Studies, and Frontier Research Center for Global Change, Japan	MIROC3.2 (medres)	1...3	1...3	1...3	K-1 Model Developers, 2004
Meteorological Institute of the University of Bonn, Germany and Institute of Korea Meteorological Administration, Korea	ECHO-G	1...3	1...3	1...3	Legutke and Voss, 1999
Max Planck Institute for Meteorology, Germany	ECHAM5/ MPI-OM	1...3	1...3	1...3	Jungclaus et al., 2006
Meteorological Research Institute, Japan	MRI-CGCM2.3.2	1...5	1...5	1...5	Yukimoto et al., 2001
National Center for Atmospheric Research, United States	CCSM3	1...4	1...3, 5...7	1...7	Collins et al., 2006
National Center for Atmospheric Research, United States	PCM	1...4	1...4	2...3	Washington et al., 2000
Hadley Center for Climate Prediction and Research/Met Office, United Kingdom	UKMO-HadCM3	1	1	1	Gordon et al., 2000
Total Number of Climate Projections		**36**	**39**	**37**	

Source: (Maurer et al., 2007)

1.2.3 Bias Correction and Spatial Downscaling

The CMIP3 climate projections have undergone BCSD to 1/8th-degree (~12-kilometer) resolution through methods described in detail in Wood et al. (2002; 2004) and Maurer (2007). The purpose of this bias correction is to adjust a given climate projection for inconsistencies between the simulated historical climate data and observed historical climate data, which are the result of GCM bias. In the BCSD approach, projections are bias corrected using a quantile mapping technique at 2-degree (~200-kilometer) spatial resolution. Following bias correction, the adjusted climate projection data are statistically consistent on a monthly basis with the observed climate data for the historical overlap period, which was 1950 to 1999 in the Study. Beyond the historical overlap period (2000 to 2099), the adjusted climate projection data reflect the same relative changes in mean, variance, and other statistics between the projected (2000 to 2099) and historical periods (1950 to 1999) as were present in the unadjusted dataset, but the adjusted climate projection data are mapped onto the observed dataset variance. This methodology assumes that the GCM biases have the same structure during the 20th and 21st Century simulations.

Downscaling spatially translates bias corrected climate data from the coarse, 2-degree (~200-kilometer), spatial resolution typical of climate models to a basin-relevant resolution of 1/8th-degree (12 kilometers), which is more useful for hydrology and other applications. The spatial downscaling process generally preserves observed spatial relationships between large- and fine-scale climates. This approach assumes that the topographic and climatic features that determine the fine-scale distribution of the large-scale climate will be the same in the future as in the historical period.

1.2.4 Weather Generation (Temporal Disaggregation)

The resulting BCSD climate projections provide a representation of future monthly temperature and precipitation through 2099. However, to be useful for hydrologic modeling, this information is required on a daily temporal scale. The monthly downscaled data were temporally disaggregated to a daily temporal scale to create realistic weather patterns using the sampling methods described in Wood et al. (2002) with extensions of this approach as applied by Salathé (2005) and Mote and Salathé (2010). To generate daily values, for each month in the simulation a month is randomly selected from the historic record for the same month (e.g., for the month of January, a January from the 1950 to 1999 period is selected). The daily precipitation and temperature from the historic record are then adjusted (rescaled precipitation and shifted temperature) such that the monthly average matches the simulated monthly value. The same historic month is used throughout the domain to preserve plausible spatial structure to daily storms (Mote and Salathé, 2010). The results of the temporal disaggregation are daily weather sequences that preserve the monthly values from the downscaled climate projections. Some uncertainties can be introduced depending on the method employed to produce the daily data from the monthly climate values. A comparative analysis of two available methods to generate daily weather patterns for the Study favored the use of the method employed by Salathé (2005) and incorporated in the SECURE Report (Reclamation, 2011) to produce the daily downscaled data. Additional detail of the comparative analysis of two daily weather generation (temporal disaggregation) methods is presented in appendix B3 under Comparison of Daily Weather Generation (Temporal Disaggregation) Methods.

2.0 Hydrologic Processes

The primary sources for hydrologic process data are derived from the VIC-simulated conditions driven by either observed historical climatology (1950 to 2005) or projected climate (1950 to 2099). VIC simulates all major moisture fluxes at the grid cell using physically based methods. These moisture fluxes are not generally measured at the spatial resolution necessary for Basin assessments; thus the VIC-derived patterns are considered the most suitable source. For example, although station-specific SWE, precipitation, and temperature are available from the National Resources Conservation Service SNOTEL network at 800 stations in 11 western states and Alaska (http://www.wcc.nrcs.usda.gov/snow/), the spatial representativeness of the SNOTEL data is uncertain (Daly et al., 2000). In preliminary results, Molotch et al. (2001) showed that SWE can begin to vary significantly beyond 500 meters from a SNOTEL site, due to terrain impacts on snow ablation, as well as small-scale depositional variations. A variety of methods have been used to distribute point measurements to spatial grids. The methods used are complex and beyond the scope of the Study; therefore, site-specific SNOTEL data were not processed to independently validate the SWE fields derived from the VIC model for the Study. However, Mote et al. (2008) found correlation of better than 0.75 between VIC-simulated SWE and measured SWE for the Rockies. Other parameters, such as ET and soil moisture, are not routinely measured, nor are they measured at scales that permit validation with the VIC-simulated fields. Thus, the use of VIC-simulated historical fluxes enables a consistent comparison of change when considering simulated fluxes under future climate.

Both the climate and hydrologic data from VIC simulations are stored in formatted text files known as "flux files." One flux file is produced for every grid cell of the model domain, and each file contains values for the specified parameters at every time step of the simulation. Gridded climate and hydrologic parameter data generated by the VIC model for the historical and projected periods were converted from daily to monthly values and stored in a specialized format (netCDF). This data conversion allows for statistical and spatial analysis of the data and enables a better understanding of the primary factors, both climatological and hydrological, that drive projected changes in streamflows relative to historical conditions. In addition to the primary VIC outputs of air temperature, precipitation, ET, runoff, and baseflow, total runoff (sum of baseflow and runoff) and runoff efficiency were computed at each grid cell and added to the netCDF files. Runoff efficiency is defined as the fraction of total runoff to the total precipitation. The complete list of hydroclimatic variables compiled is included in table B2-4.

One netCDF file was produced for each climate projection and for the historical observed data, for a total of 113 netCDF files. As with the climate data, monthly, seasonal, and annual statistics were derived for the hydrologic process information for the historical period 1971 to 2000 and three future 30-year climatological periods: 2011 to 2040, 2041 to 2070, and 2066 to 2095. The historical period 1971 to 2000 was selected as the reference climate because it was the most current 30-year climatological period described by NOAA (2010) at the time the Study was initiated. Representative statistics were generated on monthly, seasonal, and annual bases. In this analysis, the seasons are defined as follows: Fall: October, November, and December; Winter: January, February, and March; Spring: April, May, and June; and Summer: July, August, and September.

TABLE B2-4
Climate and Hydrologic Parameters

VIC Parameter	Units
Average air temperature	°C
Precipitation	millimeters (mm)
ET	mm
Runoff (surface)	mm
Baseflow (subsurface)	mm
Total runoff	mm
Soil moisture (in each of three soil layers)	mm
Soil moisture fraction	percent
SWE	mm
Runoff efficiency (total runoff/total precipitation)	fraction

The statistical analysis was conducted on both grid cell and watershed bases. The results of the grid cell analysis produce the most informative map graphics and clearly show spatial variation at the greatest resolution possible. At this spatial scale, the statistics for each grid cell are developed independently. The resulting statistics are stored in netCDF files. Monthly time series data were extracted from these files to characterize patterns of change in hydrologic parameters.

Finally, "change metrics" are generated for each parameter, in which the difference between future period statistics and historical period statistics are calculated on both absolute and percent change bases. These results are again stored in netCDF files, with two files generated for each future period—one for grid cell data and one for watershed data. The format of these files is identical to those containing the results of the statistical analysis.

3.0 Climate Teleconnections

During the past 30 years, the understanding of the climatic importance of the oceans, particularly ocean temperature, has steadily improved (U.S. Department of Interior, 2004). Initial research focused on the distant effects of the recurrent warming of the equatorial Pacific Ocean referred to as El Niño, which South American fishermen have long known to have an adverse effect on the coastal fisheries in Peru. El Niño is the warm phase of the sea-surface temperature component of a coupled ocean-atmosphere process, ENSO, which spans the equatorial Pacific Ocean. The atmospheric component, the Southern Oscillation, refers to a "seesaw" effect in sea-level pressure between the tropical Pacific and Indian Oceans. Reduced sea-level pressure in the Pacific Ocean, combined with increased sea-level pressure in the Indian Ocean, leads to a weakening in the trade winds over the eastern Pacific. This weakening enables warm water from the central equatorial Pacific to spread eastward and southward along the west coast of South America, creating the classic El Niño condition. Conversely, and about as frequently, the sea-level pressure in the Pacific Ocean increases while pressure in the Indian Ocean decreases, which causes trade winds to intensify over the eastern Pacific. When this occurs, equatorial upwelling

of deep, cold water, as well as cold water from the West Coast of South America, are pulled northward and westward from the coast into the eastern and central Pacific, producing La Niña. Thus, El Niño and La Niña are, respectively, the warm and cold phases of the coupled ENSO system.

ENSO events typically last from 6 to 18 months and, therefore, are the single most important factor affecting inter-annual climatic variability on a global scale (Diaz and Kiladis, 1992). ENSO has been linked to the occurrence of flooding in the Lower Basin (Webb and Betancourt, 1992) and to both floods and droughts across the western United States (Cayan et al., 1999). Warm winter storms have been enhanced during El Niño, causing above-average runoff and floods in the Southwest, such as during 1982 and 1983. However, not all El Niño events lead to increased runoff in the Southwest. For example, during the 2002 to 2003 warm episode, runoff was below average in the Basin. Similarly, La Niña is frequently, though not always, associated with below-average flow in the Colorado River. As a result, although ENSO exerts a strong influence in modulating wet versus dry conditions in many parts of the United States, the effect is not always the same in any given region. Some condition other than ENSO must also be influencing weather and climate patterns affecting the Colorado River.

In the mid-1990s, scientists identified another ocean temperature pattern, this one occurring in the extratropical Pacific Ocean north of 20 ºN (Mantua and Hare, 2002), the PDO. The PDO varies or oscillates on a decadal scale of 30 to 50 years for the total cycle; that is, much of the North Pacific Ocean is predominantly, though not uniformly, warm (or cool) for periods of about 15 to 25 years. During the 20th Century, the PDO exhibited several phases–warmer along coastal southeastern Alaska from 1923 to 1943 and again from 1976 to 1998, and cooler from 1944 to 1975. Since 1999, the PDO has exhibited higher-frequency fluctuations, varying from cool (1999 to 2001) to warm (2002 to 2004). Currently, the causes of the variations in the PDO are unknown and its potential predictability is uncertain. Recent research indicates that the PDO phase may be associated with decadal-length periods of above- and below-average precipitation and streamflow in the Basin (Hidalgo, 2004) but, as with ENSO, such associations are not always consistent.

Climate teleconnections were first analyzed by selecting indices that could have potential influence in streamflow changes for the Basin. Published research (Redmond and Koch, 1991; Webb and Betancourt, 1992; Cayan et al.; 1999; Mo et al., 2009; and others) indicates that the strongest correlations with Basin flows were observed with the PDO and ENSO indices. For ENSO, data were collected for both the ocean component (sea surface temperature anomalies) and the atmospheric component. The two components are highly correlated and combined describe ENSO. The SOI, the atmospheric component, was the primary dataset used in the Study due to the longer availability of information. Therefore, the quantitative teleconnections analysis was based on the PDO index and the SOI. Only a qualitative discussion of the AMO is included in the Technical Report.

Annual averages of the PDO on a water-year basis were calculated and compared with the same water year annual flows. Annual average values for the SOI were computed, using different annual windows. The average SOI index presented in the Study refers to the June to November period, which was identified as a strong indicator of ENSO events (Redmond and Koch, 1991). Once the SOI averages were computed, ENSO events were determined by years when the averaged SOI was below -1 (classified as an El Niño year) or above 1 (classified as a La Niña year). A warm PDO was defined as a PDO value greater than or equal to 0.0, and a cold PDO

was a PDO value less than 0.0. AMO research by Mo et al. (2009) indicates that the direct influence of the AMO on drought is small. The major influence of the AMO is to modulate the impact of ENSO on drought. The influence is large when the sea surface temperature anomalies in the tropical Pacific and in the North Atlantic are opposite in phase. A cold (warm) event in a positive (negative) AMO phase amplifies the impact of the cold (warm) ENSO on drought. The ENSO influence on drought is much weaker when the sea surface temperature anomalies in the tropical Pacific and in the North Atlantic are in phase. Because the AMO cycle is approximately 70 years, AMO research is constrained by the observed data record of approximately 150 years. AMO research continues in this area using indirect observations of tree rings and sedimentary layers.

There are also other climate teleconnections that appear to influence the characteristics of seasonal precipitation (e.g., Madden-Julian Oscillation and Arctic Oscillation) (Becker et al., 2011; Bond and Vecchi, 2003; Hu and Feng, 2010). However, the understanding of the influence of these teleconnections on the Colorado River precipitation, and their usefulness as an indicator, is still evolving.

4.0 Streamflow

Streamflow was analyzed through the use of two historical data sets (observed period and a longer paleo-reconstructed period) and projections of future streamflow based on climate models. Using information from the recent past, more distant past, and projections of the future enabled a robust assessment of plausible future conditions.

Two historical streamflow data sets—the observed record spanning the period 1906 to 2007 and the paleo-reconstructed record spanning the period 762 to 2005—were used in the Study to characterize historical streamflow patterns and variability. Period comparisons are made between the full extent of the data and a more recent period. For the observed dataset spanning 1906 to 2007, the second comparison period (1978 to 2007) was selected as the most recent (based on available natural flow records) 30-year period because it captures the recent drought period and the apparent climate shift after 1977 (IPCC, 2007). For the Paleo dataset spanning 762 to 2005, the second comparison period selected was 1906 to 2005 so that direct comparisons could be made of the observed and paleo timeframes. Annual flows and moving averages for 3, 5, 10, 20, and 30 years were computed for the two time periods so that differences in mean flows and variability of flows could be accessed. Annual flows and moving averages were also used to evaluate minimum and maximum streamflows. Exceedance probability plots were used to evaluate the likelihood of annual flows to exceed a specified streamflow value.

One future streamflow projection data set was represented in the Downscaled GCM Projected scenario. In this scenario, the routed streamflow from the VIC simulations driven by 112 climate projections for the period 1950 to 2099 were used to characterize natural flows at each of the 29 flow locations. VIC-simulated runoff from each grid cell was routed to the outlet of each watershed (the 29 flow locations) using VIC's offline routing tool (Lohmann et al., 1996; 1998). The routing tool processed individual cell runoff and baseflow terms and routed the flow based on flow direction and flow accumulation inputs derived from digital elevation models. Flows were output in both daily and monthly time steps. Only the monthly flows were used in the analysis for the Study. VIC routed flows are considered "natural flows" in that they do not include effects of diversions, imports, storage, or other human management of

the water resource. Bias-correction was applied to the VIC-simulated flows to account for any systematic bias in the hydrology model or data sets.

Annual streamflows for both the historical analysis and future water supply scenarios were analyzed to provide an estimate of the inter-annual variability, or deficit and surplus conditions. Definitions of "drought" are often subjective in water planning. In general, droughts are defined as periods of prolonged dryness. The inter-annual variability of the climate and hydrology of the Southwest imply basins may be in frequent states of drought. As part of the analysis conducted for this report, different averaging periods for determining and measuring deficits (cumulative volume below some reference) were considered. The definition used in the Technical Report is the following: a deficit occurs whenever the 2-year average flow falls below the long-term mean annual flow of 1906 to 2007. The use of a 1-year averaging period was discarded because it implied that any 1 year above the 15-million-acre-feet Lees Ferry natural flow would break a multi-year deficit. The use of a 2-year averaging period implies that it may take 2 consecutive above-normal years (or 1 extreme wet year) to end a drought. For a basin with sizable reservoir storage in comparison to its mean flow such as the Colorado River, it may take several years to alleviate storage deficits. Averaging periods of 1 to 10 years were evaluated, following research by Timilsena et al. (2009). The 2-year averaging period appeared to produce similar deficits as the longer-averaging periods, and was thus selected as a useful indicator.

A summary of the streamflow data sources used in each of the water supply scenarios is included below.

4.1 Observed Natural Streamflows used in the Observed Resampled Scenario

The natural streamflows were obtained for the 1906 to 2007 period at the 29 flow locations commonly used by the Reclamation for planning. Reclamation uses data collected from the U.S. Geological Survey (USGS) and other gage sites, consumptive use records, records of reservoir releases, and other data to compute monthly natural flows at 29 locations throughout the Basin: 20 locations upstream of and including the Lees Ferry gaging station in Arizona, and 9 locations below the Lees Ferry gaging station (Prairie and Callejo, 2005).

Natural flow for the Upper Basin is computed as follows:

Natural Flow = Historic Flow + Consumptive Uses and Losses+/- Reservoir Regulation

Historical streamflow data were obtained from USGS Web pages. Total depletions in the form of consumptive uses and losses include the following: irrigated agriculture, reservoir evaporation, stockponds, livestock, thermal power, minerals, municipal and industrial, and exports/imports. Reservoir regulation includes mainstem reservoirs and non-mainstem reservoirs.

Natural flows for the Lower Basin comprise computed gains and losses (on the mainstem) and historical flows (on the tributaries). Computed gains and losses consider the following consumptive uses and losses: decree accounting reports (http://www.usbr.gov/lc/region/g4000/wtracct.html), evaporation (from Lakes Mead, Mohave, and Havasu), and phreatophytes. Reservoir regulation includes change in reservoir storage and change in bank storage. Historical flows on the tributaries (Paria, Virgin, Little Colorado, and Bill Williams Rivers) have not had the historical depletions added back to the gaged flow due to the state of current methods and processes. Thus, most Lower Basin flows should not be considered natural. For more detail on

the treatment of the Lower Basin tributaries see *Technical Report C – Water Demand Assessment, Appendix C5 – Modeling of Lower Basin Tributaries in the Colorado River Simulation System*.

Monthly intervening and total natural flow for the 29 locations are available. "Intervening" flows represent the flow generated between two locations, but do not include the cumulative contribution of the locations upstream. "Total" flows, on the other hand, include the local intervening flow and all upstream flows from that location.

Additional information, documentation, and the natural flow data are available at http://www.usbr.gov/lc/region/g4000/NaturalFlow/Index.html.

4.2 Paleo Reconstructed Streamflow used in the Paleo Resampled Scenario

The natural streamflows in the Paleo Resampled scenario were derived from streamflow reconstructions at Lees Ferry from tree-ring chronologies for the period of 762 to 2005. The reconstructed streamflows at Lees Ferry were derived from ecologically contrasting tree-ring sites in the southern Colorado Plateau during the past 2 millennia (Meko et al., 2007). Streamflow values were disaggregated, spatially, and temporally, to the 29 locations by Reclamation (Prairie and Rajagopalan, 2007; Prairie et al., 2008).

4.3 Paleo Conditioned Streamflow used in the Paleo Conditioned Scenario

The Paleo Conditioned scenario blends the observed historical record and Paleo-reconstructed record to generate future inflow scenarios that comprise magnitudes of the historical record and state information from the Paleo record provided by Reclamation (Prairie and Rajagopalan, 2007; Prairie et al., 2008).

4.4 Future Streamflow Projections used in the Downscaled GCM Projected Scenario

The Downscaled GCM Projected scenario includes VIC hydrologic model traces of future streamflows for the 1950 to 2099 period from 112 GCM realizations for the 29 streamflow locations within the Basin. VIC model results were provided by Reclamation from work conducted for the West-Wide Climate Risk Assessment study (Reclamation, 2011).

5.0 References

Becker, E.J., E.H. Berbery, and R.W. Higgins. 2011. "Modulation of Cold-Season U.S. Daily Precipitation by the Madden–Julian Oscillation." *J. Climate*, 24, 5157–5166.

Bond, N. A., and G.A. Vecchi. 2003. "The influence of the Madden–Julian oscillation on precipitation in Oregon and Washington." *Wea. Forecasting*, 18, 600–613.

Bureau of Reclamation (Reclamation). 2010. Colorado River Natural Flow and Salt Data. Retrieved December 2010, from http://www.usbr.gov/lc/region/g4000/NaturalFlow/supportNF.html.

Bureau of Reclamation (Reclamation). 2011. *SECURE Water Act Section 9503(c) – Reclamation Climate Change and Water 2011*.

Cayan, D.R., K.T. Redmond, and L.G. Riddle.1999. "ENSO and Hydrologic Extremes in the Western United States." *Journal of Climate*, 12: 2881-2893.

Collins, W.D., C.M. Bitz, M.L. Blackmon, G.B. Bonan, C.S. Bretherton, J.A. Carton, P. Chang, S.C. Doney, J.J. Hack, T.B. Henderson, J.T. Kiehl, W.G. Large, D.S. McKenna, B.D. Santer, and R.D. Smith. 2006. "The Community Climate System Model Version 3 (CCSM3)." *J Climate*, 19(11):2122-2143.

Daly, C., G.H. Taylor, W. P. Gibson, T.W. Parzybok, G. L. Johnson, and P. Pasteris. 2000. "High-quality spatial climate data sets for the United States and beyond." *Transactions of the American Society of Agricultural Engineers*, 43**:** 1957-1962.

Diaz, H.F., and G.N. Kiladis. 1992. "Atmospheric Teleconnections Associated with the Extreme Phases of the Southern Oscillation." Diaz, H.F., and V.A. Markgraf (eds.), *El Niño: Historical and Paleoclimatic Aspects of the Southern Oscillation.*

Diansky, N.A., and E.M. Volodin. 2002. "Simulation of present-day climate with a coupled atmosphere-ocean general circulation model." *Izv Atmos Ocean Phys* (English translation) 38(6):732-747.

Delworth, T.L., et al. 2006. GFDL's CM2 global coupled climate models part 1: formulation and simulation characteristics. *J Climate* 19:643-674.

Furevik, T., M. Bentsen, H. Drange, I.K.T. Kindem, N.G. Kvamstø, and A. Sorteberg. 2003. "Description and evaluation of the bergen climate model: ARPEGE coupled with MICOM." *Clim Dyn* 21:27-51.

Flato, G.M., and G.J. Boer. 2001. "Warming Asymmetry in Climate Change Simulations." *Geophys. Res. Lett.*, 28:195-198.

Gordon C., C. Cooper, C.A. Senior, H.T. Banks, J.M. Gregory, T.C. Johns, , J.F. B. Mitchell, and R.A. Wood. 2000. 'The simulation of SST, sea ice extents and ocean heat transports in a version of the Hadley Centre coupled model without flux adjustments." *Clim Dyn* 16:147-168.

Hidalgo, H. G. 2004. "Climate precursors of multi-decadal drought variability in the western United States" *Water Resour. Res.*, 40, W12504, DOI:10.1029/2004WR003350.

Hu, Q., and S. Feng. 2010. "Influence of the Arctic oscillation on central United States summer rainfall." *J. Geophys. Res.*, 115, D01102. DOI: 10.1029/2009JD011805.

Institut Pierre Simon Laplace. 2005. "The new IPSL climate system model: IPSL-CM4." *Institut Pierre Simon Laplace des Sciences de l'Environnement Global*.

Intergovernmental Panel on Climate Change (IPCC). 2000. *Emissions Scenarios. Special Report of the Intergovernmental Panel on Climate Change* [Nakicenovic, N., and R. Swart, (eds.)].

Intergovernmental Panel on Climate Change (IPCC). 2007. *Climate Change 2007: The Physical Science Basis. Contribution of Working Group I to the Fourth Assessment Report of the Intergovernmental Panel on Climate Change* [Solomon, S., D. Quin, M. Manning,, Z. Chen, M. Marquis, K.B. Averyt, M. Tignor, and H.L. Miller, (eds.)].

Joint Institute for the Study of the Atmosphere and Ocean. 2010. Retrieved Marh 30, 2011 from http://jisao.washington.edu/pdo/.

Jungclaus, J.H., M. Botzet, H. Haak, N. Keenlyside, J-J Luo, M. Latif, J. Marotzke, U. Mikolajewicz, and E. Roeckner. 2006. "Ocean circulation and tropical variability in the AOGCM ECHAM5/MPI-OM." *J Climate* 19:3952-3972.

K-1 Model Developers. 2004. "K-1 coupled model (MIROC) description, K-1 technical report, 1." In: *Frontier Research Center for Global Change*. Hasumi, H., Emori, S. (eds). Center for Climate System Research

Legutke, S., and R. Voss. 1999. *The Hamburg Atmosphere-Ocean Coupled Circulation Model ECHO-G. Technical report, No. 18*.

Lohmann, D., R. Nolte-Holube, and E. Raschke. 1996. "A large-scale horizontal routing model to be coupled to land surface parameterization schemes." *Tellus*, 48: 708-721.

Lohmann, D., E. Raschke, B. Nijssen, and D.P. Lettenmaier. 1998. "Regional Scale Hydrology: I. Formulation of the VIC-2L Model Coupled to a Routing Model." *Hydrological Sciences Journal*, 43, 131-141.

Mantua, N.J., and S.R. Hare, S.R. 2002. "The Pacific Decadal Oscillation." *Journal of Ocean*, 58: 35-42.

Maurer, E.P. 2007. "Uncertainty in hydrologic impacts of climate change in the Sierra Nevada, California under two emissions scenarios." *Climatic Change*, Vol. 82, No. 3-4, 309-325, DOI: 10.1007/s10584-006-9180-9.

Maurer, E. P., L. Brekke, T. Pruitt, and P.B. Duffy. 2007. "Fine-Resolution Climate Projections Enhance Regional Climate Change Impact Studies." *Eos, Transactions, American Geophysical Union*, 88 (47), 504.

Maurer, E.P., A.W. Wood, J.C. Adam, D.P. Lettenmaier, and B. Nijssen. 2002. "A Long-Term Hydrologically-Based Data Set of Land Surface Fluxes and States for the Conterminous United States." *Journal of Climate*, 15(22), 3237-3251.

Meko, D.M., C.A. Woodhouse, C.A. Baisan, T. Knight, J.J. Lukas, M.K. Hughs, and M.W. Salzer. 2007. "Medieval Drought in the Upper Colorado River Basin." *Geophysical Research Letters*, 34(5), L10705, DOI: 10.1029/2007GL029988.

Mo, K.C., J.E. Schemm, and S. Yoo. 2009. "Influence of ENSO and the Atlantic Multi-Decadal Oscillation on Drought over the United States." *Journal of Climate*, 22(22), 5962-5982. DOI:10.1175/2009JCLI2966.1.

Mote, P., M. Clark, and A. Hamlet. 2008. "Variability and Trends in Mountain Snowpack in Western North America. 20th Conference on Climate Variability and Change". American Meteorological Society. New Orleans, Louisiana.

Mote P.W., and E.P. Salathé. 2010. "Future climate in the Pacific Northwest." *Climatic Change*, 102, 29–50. DOI 10.1007/s10584-010-9848-z.

Molotch, N. P., S.R. Fassnacht, M.T. Colee, T. Bardsley, and R.C. Bales. 2001. "A comparison of spatial statistical techniques for the development of a validation dataset for mesoscale modeling of snow water equivalence." *Eos Trans*. AGU, 82(47), Fall Meet. Suppl., F553.

National Oceanic and Atmospheric Administration (NOAA). 2010. Retrieved June 30, 2011, from http://www.ncdc.noaa.gov/oa/climate/normals/usnormalsprods.html.

National Oceanic and Atmospheric Administration (NOAA). 2011. Retrieved June 30, 2011, from http://www.ncdc.noaa.gov/oa/climate/normals/usnormals.html.

National Resources Conservation Service. 2011. Retrieved June 30, 2011 from http://www.wcc.nrcs.usda.gov/snow/.

Prairie, J., and R. Callejo. 2005. *Natural Flow and Salt Computation Methods, Calendar Years 1971-1995*. U.S. Department of the Interior, Bureau of Reclamation, Salt Lake City, Utah, Boulder City, Nevada.

Prairie, J., and B. Rajagopalan. 2007. "Stochastic Streamflow Generation Incorporating Paleo-Reconstruction." Proceedings of the World Environmental and Water Resources Congress, Tampa, Florida.

Prairie, J., K. Nowak, B. Rajagopalan, U. Lall, and T. Fulp. 2008. "A Stochastic Nonparametric Approach for Streamflow Generation Combining Observational and Paleoreconstructed Data." *Water Resources Research.* Vol. 44, W06423, DOI: 10.1029/2007WR006684.

Russell, G.L., J.R. Miller, D. Rind, R.A. Ruedy, G.A. Schmidt, and S. Sheth. 2000. "Comparison of model and observed regional temperature changes during the past 40 years." *J Geophys Res* 105:14891-14898.

Redmond, K.T., and R.W. Koch. 1991. "Surface Climate and Streamflow Variability in the Western United States and Their Relationship to Large-Scale Circulation Indices." *Water Resources Research*, 27, 2381–2399.

Salathé, E.P. 2005. "Downscaling simulations of future global climate with application to hydrologic modeling." *Int J Climatol*, 25, 419–436.

Salas-Mélia, D., F. Chauvin, M. Déqué, H. Douville, J.F. Gueremy, P. Mareut, , S. Planton, J.F. Royer, and S. Tyteca. 2005. "Description and validation of the CNRM-CM3 global coupled model, CNRM working note 103."

Timilsena J., T. Piechota, G. Tootle, and A. Singh. 2009. "Associations of interdecadal/interannual climate variability and long-term Colorado River Basin streamflow." *J. Hydrol*. 365(3-4), 289-301, DOI:10.1016/j.jhydrol.2008.11.

U.S. Department of the Interior. 2004. "Climatic Fluctuations, Drought, and Flow in the Colorado River Basin, U.S. Geological Survey." *USGS Fact Sheet 2004-3062*, version 2.

University of East Anglia Climatic Research Unit. 2010. Retrieved March 30, 2011 from http://www.cru.uea.ac.uk/cru/data/soi/.

Washington W.M., J.W. Weatherly, G.A. Meehl, A.J. Semtner, T.W. Bettge, A.P. Craig, W.G. Strand, J. Arblaster, V.B. Wayland, R. James, Y. Zhang. 2000. "Parallel climate model (PCM) control and transient simulations." *Clim Dyn* 16:755-774.

Webb, R.H., and J.L. Betancourt. 1992. "Climatic Variability and Flood Frequency of the Santa Cruz River, Pima County, Arizona: U.S. Geological Survey." *Water-Supply Paper 2379*.

Wood, A.W., E.P. Maurer, A. Kumar, and D.P. Lettenmaier. 2002. "Long-range experimental hydrologic forecasting for the Eastern United States." *J. Geophysical Research-Atmospheres*, 107(D20), 4429, DOI:10.1029/ 2001JD000659.

Wood, A.W., L.R. Leung, V. Sridhar, and D.P. Lettenmaier. 2004. "Hydrologic implications of dynamical and statistical approaches to downscaling climate model outputs." *Climatic Change*, 15, 189–216.

Yukimoto S., A. Noda, A. Kitoh, M. Sugi, Y. Kitamura, M. Hosaka, K. Shibata, S. Maeda, and T. Uchiyama. 2001. "The new Meteorological Research Institute coupled GCM (MRI-CGCM2) – model climate and variability." *Pap Meteorol Geophys* 51:47-88.